Nuclear Instruments and Methods in Physics Research A238 (1985) 347–353
North-Holland, Amsterdam

A LOGARITHMIC DETECTION SYSTEM SUITABLE FOR A 4π ARRAY

G.D. WESTFALL, J.E. YURKON, J. VAN DER PLICHT, Z.M. KOENIG, B.V. JACAK, R. FOX, G.M. CRAWLEY, M.R. MAIER and B.E. HASSELQUIST

National Superconducting Cyclotron Laboratory, Michigan State University, East Lansing, MI 48824, USA

R.S. TICKLE

Department of Physics, University of Michigan, Ann Arbor, Michigan 48109, USA

D. HORN

Atomic Energy of Canada Limited, Chalk River Nuclear Laboratory, Chalk River, Ontario, Canada, K0J1J0

Received 28 January 1985

A low pressure multiwire proportional counter, a Bragg curve counter, and an array of CaF_2/plastic scintillator telescopes have been developed in a geometry suitable for close packing into a 4π detector designed to study nucleus–nucleus reactions at 100–200 MeV/nucleon. The multiwire counter is hexagonal in shape and gives $X-Y$ position information using resistive charge division from nichrome-coated stretched polypropylene foils. The Bragg curve counter is a hexagonal pyramid with the charge taken from a Frisch gridded anode. A field shaping grid gives the Bragg curve counter a radial field. The scintillator telescopes are shaped as truncated triangular pyramids such that when stacked together they form a truncated hexagonal pyramid. The light signal of the CaF_2–plastic combination is read with one phototube using a phoswich technique to separate the ΔE signal from the E signal. The entire system has been tested so far for particles with $1 \leqq Z \leqq 18$ and gives good position, charge, and time resolution.

1. Introduction

High energy nucleus–nucleus collisions at energies above 200 MeV/nucleon have been studied with detection systems designed to measure one light particle (π, n, p, d, t, ^{3}He and ^{4}He) or a few light particles from each interaction [1–4]. Recent experimental results [5,6] demonstrate that to differentiate between the predictions of various models such as hydrodynamics, cascade, and thermal, one must measure as many of the outgoing particles as possible. Several systems have been developed to deal with large multiplicities of light charged particles emerging from high energy nucleus–nucleus collisions. These include the Plastic Ball [7], the streamer chamber [8], the time projection chamber (TPC) [9], HISS [10], and DIOGENE [11]. At energies below 200 MeV/nucleon, the problem of detecting multi-particle final states is complicated by the increasing importance of heavy fragments (Li, Be, B, etc.) [12] and is made easier by the smaller multiplicity of emitted particles.

The simultaneous detection of all types of charged particles ranging from pions to fission fragments requires a system with a very large dynamic range. One way to obtain 4π coverage and retain a large dynamic range is to construct an apparatus that has a logarithmic increase in the stopping power of the detector as a function of the range of the emitted particle. Presented here are the prototypes for the detectors that will form such a system.

The low pressure multiwire proportional counter – (LP)MWPC – makes up the inner layer and is capable of detecting fission fragments and other slow, highly ionizing particles around Coulomb barrier energies. The MWPC provides position sensitivity as well as timing information for these particles. The Bragg curve counter (BCC) is designed to detect more energetic particles such as ^{12}C nuclei at 30 MeV and functions as the more dense second layer. The BCC gives the Z and total energy of fragments that stop in it. A Bragg curve counter was chosen, rather than a standard ion chamber with the electric field perpendicular to the particle paths, because it lends itself more readily to close packing and the output consists of one signal. Penetrating light particles will pass completely through MWPC and BCC and can be observed in scintillator telescopes. The scintillator telescopes provide ΔE–E information for ligh particles such as pions, protons, and alphas as well as timing information for random-coincidence suppression and pion identification. Both signals are read out with a single photomultiplier tube, the slow CaF_2 and fast

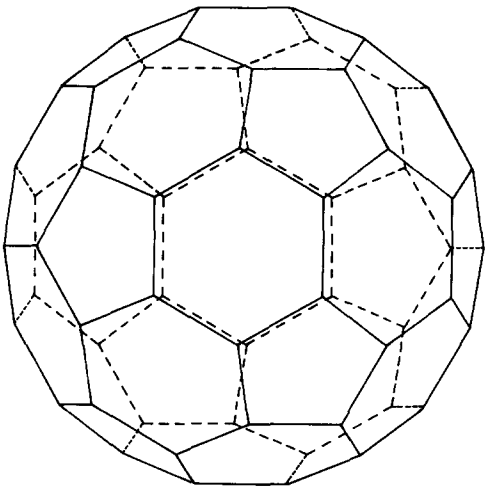

Fig. 1. A 32 face truncated icosahedron, consisting of 20 hexagons and 12 pentagons.

plastic signals being separated using different time gates on the output signal.

The requirement of covering a large fraction of 4π with MWPCs, BCCs, and scintillator telescopes constrains the shape of the detectors. The shape chosen is based on a thirty two face truncated icosahedron containing 20 regular hexagonal faces and 12 regular pentagonal faces. An example of this geometrical object is shown in fig. 1 with the hidden lines shown dashed. The geometry of the counters presented here (the prototype subarray) is a truncated hexagonal pyramid and is shown schematically in fig. 2. Another aspect of attempting to cover a solid angle close to 4π is that the detector must be sensitive over most of its area and must have walls that present a small cross section compared to the active area. The detector is constructed such that the center lines of the walls are along radii of a sphere centered at the target.

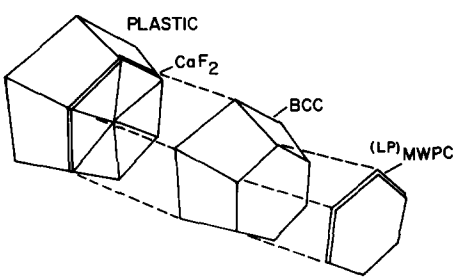

Fig. 2. Schematic representation of one of the 30 subarrays that will make up the multiparticle array.

2. Apparatus

We have constructed and succesfully tested one prototype subarray (i.e. one MWPC and BCC, followed by 6 scintillator telescope elements) as is shown in fig. 2. The distance from the target to the center of the front of the MWPC is 15 cm. The active area of the MWPC is 65 cm^2 giving a solid angle of 0.29 sr. The total thickness of the MWPC including support frames is 1.6 cm and the total length of the BCC is 15 cm. The thickness of the prototype scintillator telescope is 3 mm for the CaF_2 and, at present, 15 cm for the plastic.

2.1. The MWPC

The MWPC is a low pressure gas detector utilizing the double amplification process as discovered by Breskin et al. [13]. Based on this principle, detectors have been built with active areas of 2×2 cm^2 which have an intrinsic time resolution of 100 ps. These devices can be used as start detectors for heavy and slowly moving particles such as fission fragments [14]. Also, larger versions (8×10 cm^2 area) of low pressure MWPCs have been developed, and made position sensitive in two dimensions by dividing the cathode foils into strips [15]. However, because this method requires components such as delay lines outside the detector body, this method of position readout is impractical for applications requiring close-packing. For this reason the strips on the cathode foils were connected by a resistive NiCr strip as described below. The position signal is then obtained by the charge division method.

The detector is shown in exploded view in fig. 3. The anode is a plane in the center of the detector composed of gold plated tungsten wires 12 μm in diameter spaced 1 mm apart. These wires are connected to the high voltage and also provide a fast timing signal. The two

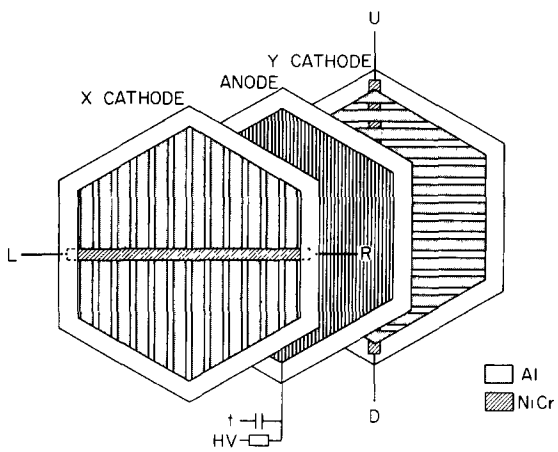

Fig. 3. Exploded view of the hexagonal MWPC.

cathodes are at ground potential and are located 3.2 mm from the wire plane. Each cathode plane consists of a polypropylene foil, stretched to a thickness of about 75 $\mu g/cm^2$. The cathode foils are coated with a resistive strip of nichrome (nickel/chrome 80/20%). This NiCr strip in turn is coated with 5 mm wide Al strips perpendicular to the NiCr strip as indicated in fig. 3. The resistance between the end contacts of the cathode foils is typically in the range of 1–5 kΩ. The orientation of one striped cathode (say X) is 90° with respect to the second (Y). From each cathode, the position is calculated by the data-acquisition computer with the charge division method, i.e. $X = L/(L + R)$ and $Y = U/(U + D)$. Here L, R, U, D symbolize the left, right, up and down signals.

The support frames are made from G10 fiberglass epoxy laminate and are sealed with silicone rubber gaskets. The pressure window is also a 75 $\mu g/cm^2$ stretched polypropylene foil supported by three stainless steel wires across the entrance of the detector. The MWPC is designed to operate at a pressure of 2 Torr isobutane gas.

2.2. The BCC

A Bragg curve counter (BCC) is basically an ionization chamber with its field parallel to the incoming particles. In this way the range of the particles that are stopped in the detector can be measured. The idea of a Bragg curve counter was originally put forth by Gruhn et al. who also constructed the first operational BCC [16]. Since that time several groups have constructed BCCs along similar lines [17–20]. The BCC takes advantage of the fact that the maximum specific ionization of a stopping ion is proportional to the atomic number of the particle. By measuring the maximum of the ionization one obtains the charge Z of the particle; the integral of the ionization is a measure of the energy E. In principle, since one has obtained multiple ΔE measurements, the mass A of the particle should also be accessible (see e.g. ref. [20]).

The electrons liberated by the ionization of the stopping charged particle drift to an anode which is shielded by a Frisch grid. Since the electric field is parallel to the path of the particle, one measures the charge collected on the anode as a function of time, and thus obtains the complete energy loss distribution of the stopping ion. In the present counter the range of subtended angles to be covered is very large and the information concerning the ionization of the stopping particles will be lost if the electrons do not drift parallel to the trajectory of the particle. Thus, a field shaping grid was installed inside the BCC to approximate a radial field. This is illustrated in fig. 4. The design of this field shaping grid was calculated with the program POISSON [21] in cylindrical geometry.

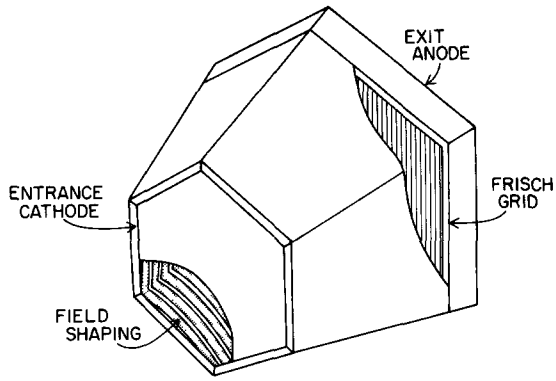

Fig. 4. Schematic view of the Bragg curve counter.

The main structure of the BCC is a hexagonal pyramid made from 6.35 mm G10 fiberglass epoxy laminate. The entrance window of the BCC has a minor diameter of 10 cm. The pressure window of the BCC is made of 6 μm (or 800 $\mu g/cm^2$) thick aluminized mylar supported by a wire grid with 1 cm spacing. The distance between the cathode and the Frisch grid is 14 cm. The Frisch grid is made of 12.5 μm gold plated tungsten wires with a 0.5 mm spacing. The anode is a similar wire grid located 1 cm behind the Frisch grid. The rear pressure window is formed by the scintillator telescopes. The BCC usually operates at a pressure of 500 Torr Ar/CH_4 (90/10%) gas.

2.3. The scintillator telescopes

The scintillator telescopes are designed to detect light particles from pions to alphas. The basic technique for obtaining ΔE and E information for particle identification and energy measurement is a "phoswich" technique originally suggested by Wilkinson [22] and recently put into regular use by Gutbrod et al. [7]. This technique takes advantage of the different time constants for the emission of scintillation light from CaF_2 crystals and from plastic scintillators. We used 3 mm thick CaF_2(Eu) [23] crystals for the ΔE scintillator, and 15 cm thick BC412 [24] plastic scintillator for the E. The characteristic time for light emission from CaF_2 is 1 μs while plastic scintillators emit most of their light in 50 ns. Thus one can obtain the energy loss in a thin CaF_2 ΔE detector by putting a long, delayed gate on the output signal of the phototube while the energy deposited in the plastic scintillator is obtained using a prompt, short gate.

The geometry of the scintillation counters aids this technique because the collection efficiency for the light produced by the CaF_2 is higher than light produced near the back for the plastic scintillator giving a satisfactory ratio of the light emitted by the two different scintillators. The 6 scintillator telescopes are each con-

nected via lightguides to Philips XP2202 photomultipliers. The light emission of CaF_2 is about the same as that for anthracene, and that of the plastic (BC412), about 60% of anthracene.

3. Results of test experiments

The detector elements of the prototype array have been tested extensively, both with radioactive sources (where possible) and with heavy-ion beams. Experiments were performed with beams of 360 MeV ^{12}C and 490 MeV ^{14}N at the National Superconducting Cyclotron Laboratory of Michigan State University, with 230 MeV ^{35}Cl at the tandem/linac accelerator of Argonne National Laboratory, and with 4 GeV ^{40}Ar at the Bevalac of Lawrence Berkeley Laboratory.

3.1. The MWPC

We present her tests of the MWPC as performed with a ^{252}Cf(sf) source. The time resolution has been checked by measuring the time of flight of fission fragments between a "normal" MWPC type startdetector (such as reported in ref. [14]) and the hexagon type MWPC positioned behind it. The total resolution obtained this way for fission fragments was about 600 ps fwhm. The intrinsic resolution for elastic scattering of high energy heavy ions is expected to be better than 200 ps [15]. A two-dimensional plot of X-position versus Y-position is shown in fig. 5. The plot shows the detector, exposed to fission fragments from the ^{252}Cf source through a mask. The mask consists of a hexagon, covering the whole of the detector except an outer rim of about 1.5 mm and a lettering pattern. We concluded that the position resolution of the hexagonal MWPC in both dimensions is better than 1 mm fwhm. The right part of the plot appears more compressed than the left part. This is due to a non-uniform evaporation of the NiCr strip on this cathode foil, causing a change in resistance going from one end to the other.

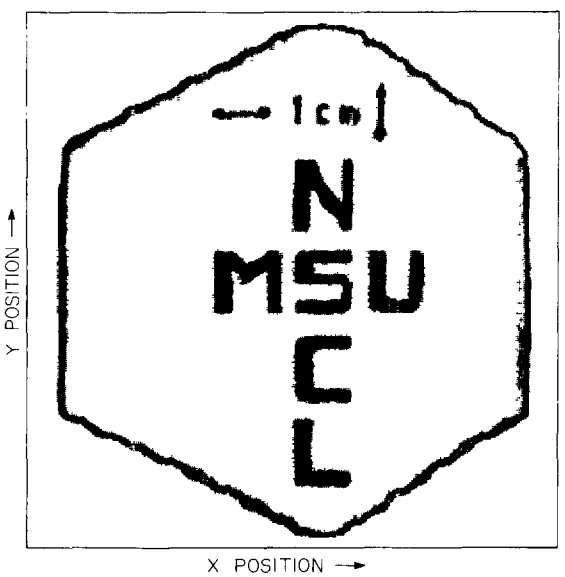

Fig. 5. Contour plot of a two-dimensional MWPC position spectrum, showing horizontal (X-axis) vs vertical (Y-axis) position.

3.2. The BCC

The Bragg curve counter can be read out using two different techniques. Firstly, from the measured Bragg curve the peak amplitude and the total energy can be deduced with amplifiers having short and long shaping times, respectively. Secondly, the particle can be followed through its Bragg curve as a function of time using a flash ADC.

Fig. 6 shows results as obtained with a beam of 35 MeV/A ^{14}N delivered by the superconducting cyclotron of NSCL/MSU. Heavy fragments resulting from the reaction Au(^{14}N, X) were detected. The detector was placed at an angle of 45°. The first (analog) readout method was used in this case. The anode signal of the BCC was, after amplification by a charge sensitive preamplifier, distributed to two spectroscopy amplifiers. One of these amplifiers was set at a time constant of

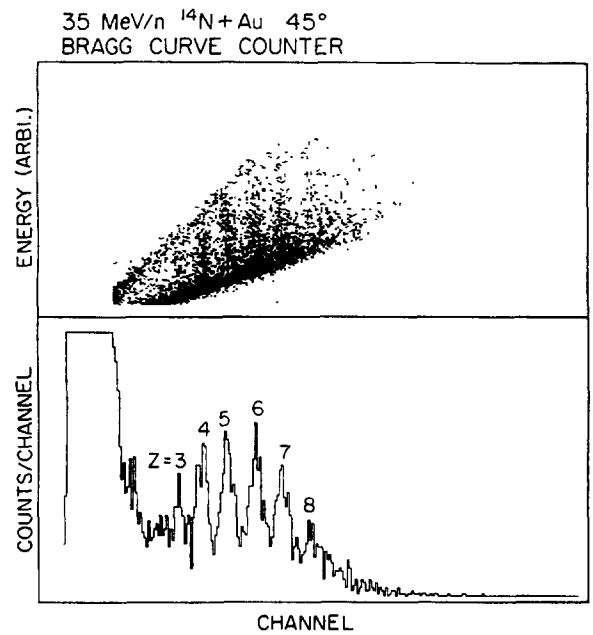

Fig. 6. Top: two-dimensional plot of Z (horizontal) vs E (vertical) for the reaction $^{14}N + ^{197}Au$ at 35 MeV/A. Bottom: projected Z spectrum for the same reaction.

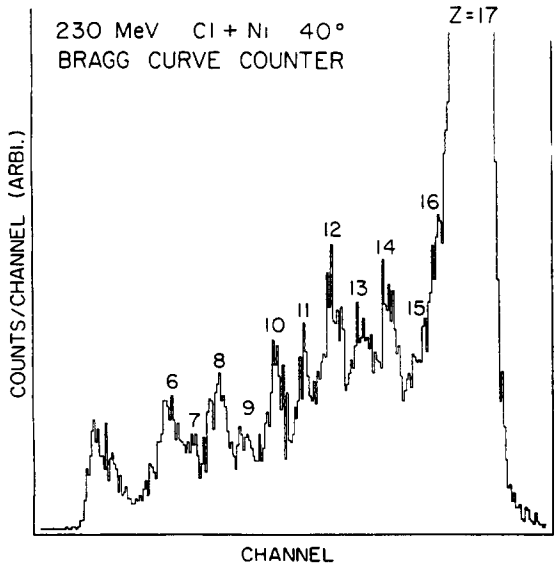

Fig. 7. Charge spectrum for the reaction $^{35}Cl+^{58}Ni$ at 230 MeV.

0.25 μs and therefore measures the charge Z of the ion; the other one was set at a time constant of 6 μs and therefore measured the energy E.

The top part of fig. 6 shows a two-dimensional plot of the charge Z (horizontal axis) versus E (vertical axis). The bottom part of fig. 6 shows the one-dimensional projection (Z-spectrum) of the same reaction. The charges are indicated. Another example obtained for higher charges is shown in fig. 7. Results from the

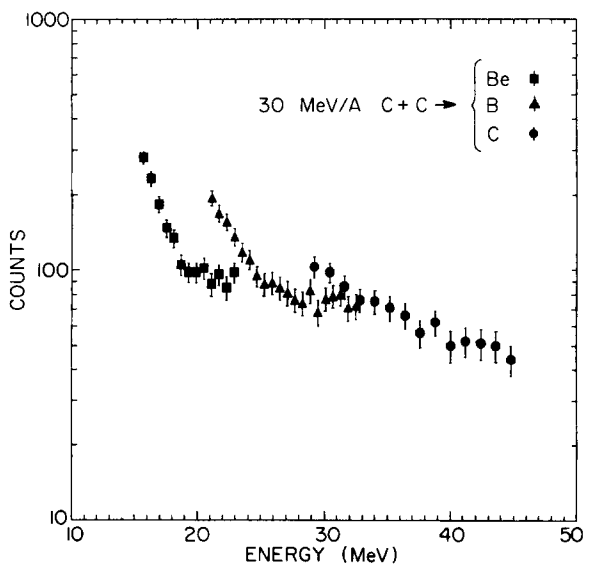

Fig. 8. Energy spectra for Be, B and C fragments from the reaction $^{12}C+^{12}C$ at 30 MeV/A, as measured with the Bragg curve detector.

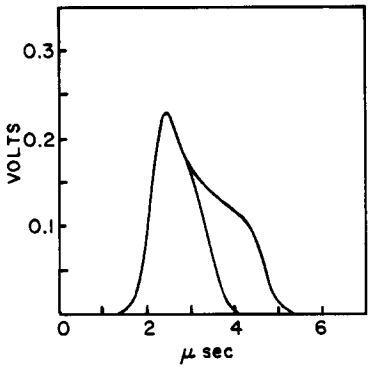

Fig. 9. Bragg curves for α-particles from a ^{228}Th source, as observed on an oscilloscope.

reaction $^{35}Cl+^{58}Ni$ are presented. The beam of 230 MeV ^{35}Cl was provided by the Argonne tandem/linac accelerator. Charges up to $Z=17$ are observed in this case.

In the two-dimensional Z versus E plots, the Z lines usually appear slightly curved, and more so near the "punch-through" line. This effect is discussed in detail in ref. [25]. Despite these effects, the individual charges remain resolved and can be isolated using two-dimensional contour gates. The spectra shown in the bottom of fig. 6 and in fig. 7 are not corrected for these nonlinearities. As an illustration of charges separation, we show in fig. 8 energy spectra for Be, B and C fragments resulting from the reaction $^{12}C+^{12}C$ at 30 MeV/nucleon. To obtain the energy calibration, we used the lines which show up in the Z versus E plot

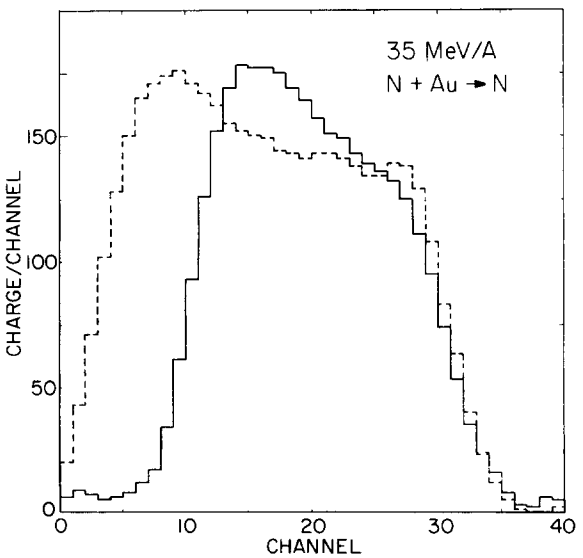

Fig. 10. "Snapshot" of the BCC, i.e. the digitized current output as measured with the flash encoder.

and correspond to fragments that barely make it into the detector, and to fragments that punch through. The particles with energies in the vicinity of these extremes are excluded (with a software gate). This calibration is linear to a good approximation (see ref. [25]). The energy loss through the pressure windows is taken into account.

The current signal of the BCC for α particles from a ^{228}Th source is shown in fig. 9. The signal was amplified by a timing filter amplifier. The Bragg curves for the two main α-lines (6.09 and 8.78 MeV) are clearly visible. The second method of reading out the BCC utilizes this current signal. This signal is digitized by a flash encoder that integrates the charge in 30–100 ns time bins. Again, the peak of the distribution can be related directly to the Z of the passing ion, and the integral of the curve is the total energy. Typical Bragg curves (snapshots), obtained this way for the reaction ^{14}N + Au at 35 MeV/nucleon, are shown in fig. 10. The two curves shown correspond to N fragments of different energies. Note that the two curves show the same peak height (corresponding to Z) but different areas (corresponding to E). The X-axis of fig. 10 corresponds to time; the time actually runs from right to left since the readout is done from the anode. The calibration is 90 ns/channel.

3.3. The scintillator telescopes

We present here results on the CaF_2/plastic $\Delta E/E$ telescopes as obtained at NSCL with the reaction ^{12}C + ^{12}C at a beam energy of 30 MeV/A. In fig. 11, a two-dimensional plot of ΔE versus E is shown. The light particles resulting from the nuclear collision (p, d, t, ^{3}He, α) are clearly identified. The prompt gate on the plastic E scintillator was about 50 ns wide, whereas the gate on the CaF_2 ΔE scintillator was about 1 μs wide.

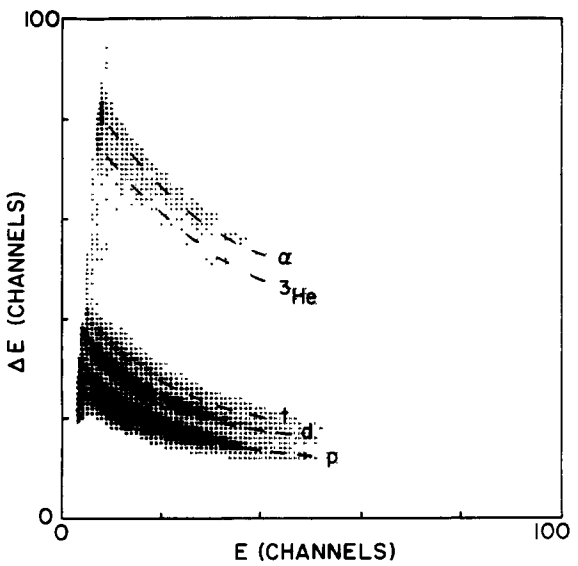

Fig. 11. Contour plot of ΔE (vertical) vs E (horizontal) for the CaF_2/plastic scintillator telescope. The reaction is ^{14}N + Au at 35 MeV/A.

4. Conclusions

A logarithmic detector for nuclear experiments with up to about 200 MeV/nucleon beam energies has been built. It consists of a stack containing a low-pressure MWPC for slow and heavy fragments, a Bragg curve spectrometer for intermediate energy fragments and CaF_2/plastic scintillator telescopes for light particles.

This detector array is a hexagonally shaped cone and is a prototype element for a device with a solid angle close to 4π.

Results of initial test experiments of this multi-particle detector with a variety of heavy-ion beams are reported. These results demonstrate its suitability for use as the basic building block of a 4π array. Such an array is presently under construction at our laboratory.

Appendix

Most scintillator telescopes that utilize the phoswich technique consist of a CaF_2 ΔE element, and plastic E element. This includes the prototype detector for the 4π array described in this paper. Recently, however a new plastic with a slow decay time constant has been developed [26]. The properties of this new plastic scintillator, compared with CaF_2 and the regular "fast" plastic are shown in table 1.

We are presently planning to use a "fast/slow" plastic phoswich detector for the 4π detector. The advantages as compared to the CaF_2 (slow)/plastic (fast) system are:

1) much easier to machine than CaF_2 in the desired shapes (hexagonally and pentagonally shaped cones);
2) the index of refraction of both scintillators are the same providing ideal optical coupling;

Table 1
Properties of three scintillator materials

	Fast plastic BC412	Slow plastic BC444	CaF_2
Density (g/cm^3)	1.032	1.032	3.19
Peak emission (nm)	434	428	435
Decay constant (ns)	3.3	180	940
Refraction index	1.58	1.58	1.44
Light yield (%antracene)	60	41	100

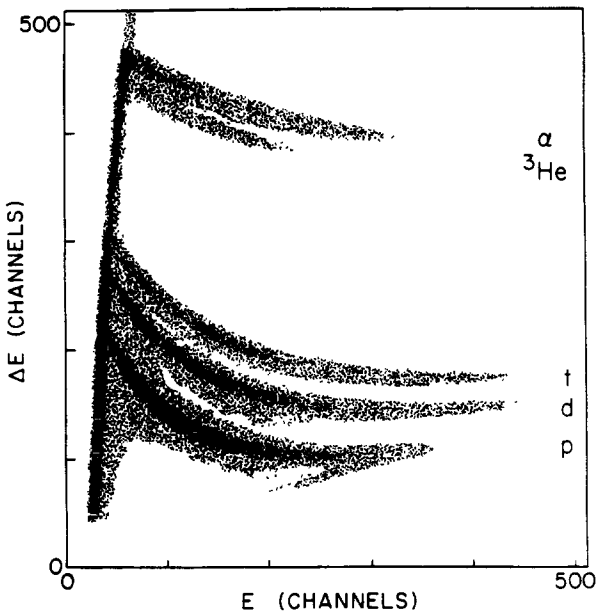

Fig. 12. Particle identification spectrum for a "fast/slow" scintillator phoswich telescope.

3) the thin ΔE scintillator is the fast one (as opposed to the CaF_2/plastic system) defining a better electronic trigger signal.

We tested a sample "fast/slow" detector. The ΔE detector consisted of a 6.4 mm thick BC444 slow plastic, the E detector of 5 cm BC412 fast plastic. The diameter of the scintillators was 5 cm. This scintillator telescope was read out using a R329 photomultiplier. The telescope was placed at a laboratory angle of about 20°, and particles from the reaction $^{12}C + ^{197}Au$ at 30 MeV/nucleon were detected. The beam was delivered by the superconducting cyclotron of NSCL/MSU. The gate width for the fast component was set at 40 ns wide, and for the slow component 1 μs. The resulting $\Delta E/E$ plot is shown in fig. 12. As can be seen, the particle identification properties are excellent. Light particles (p, d, t, ^{3}He, α) are observed with energies corresponding to the thickness of the scintillator telescope elements. The ΔE detector provides the trigger signal. For the protons, particles that "punch through" the detector are visible. The peak-to-background ratio for the protons is about 500 to 1.

References

[1] J. Gosset, H.H. Gutbrod, W.G. Meyer, A.M. Poskanzer, A. Sandoval, R. Stock and G.D. Westfall, Phys. Rev. C16 (1977) 629.

[2] A. Sandoval, H.H. Gutbrod, W.G. Meyer, R. Stock, Ch. Lukner, A.M. Poskanzer, J. Gosset, J.-C. Jourdain, C.H. King, Nguyen Van Sen, G.D. Westfall and K.L. Wolf, Phys. Rev. C21 (1980) 1321.

[3] S. Nagamiya, M.-C. Lemaire, E. Moeller, S. Schnetzer, G. Shapiro, H. Steiner and I. Tanihata, Phys. Rev. C24 (1981) 971.

[4] G.D. Westfall, B.V. Jacak, N. Anantaraman, M.W. Curtin, G.M. Crawley, C.K. Gelbke, B. Hasselquist, W.G. Lynch, D.K. Scott, M.B. Tsang, M.J. Murphy, T.J.M. Symons, R. Legrain and T.J. Majors, Phys. Lett. 116B (1982) 118.

[5] H.H. Gutbrod, H. Löhner, A.M. Poskanzer, T. Renner, H. Riedesel, H.G. Ritter, A. Warwick, F. Wiek and H. Wieman, Phys. Lett. 127B (1983) 317.

[6] H. Ströbele, R. Brockmann, J.W. Harris, F. Riess, A. Sandoval, R. Stock, K.L. Wolf, H.G. Pugh, L.S. Schroeder, R.E. Renfordt, K. Tittel and M. Maier, Phys. Rev. C27 (1983) 1349.

[7] A. Baden, H.H. Gutbrod, H. Lohner, M.R. Maier, A.M. Poskanzer, T. Renner, H. Riedesel, H.G. Ritter, H. Spieler, A. Warwick, F. Weik and H. Wieman, Nucl. Instr. and Meth. 203 (1982) 189.

[8] Proc. 1st Int. Conf. on Streamer Chamber Technology, Argonne, ed., J.M. Watson, ANL-8055 (1972).

[9] D. Fancher, H.J. Hilke, S. Loken, P. Martin, J.N. Marx, D.R. Nygren, P. Robrish, G. Shapiro, M. Urban, W. Wenzel, W. Gorn and J. Layter, Nucl. Instr. and Meth. 161 (1979) 383.

[10] D.E. Greiner, Nucl. Phys. A400 (1983) 325.

[11] J. Gosset, Workshop on Future relativistic heavy-ion experiments, Darmstadt (1980) GSI 81-6, p. 441.

[12] B. V. Jacak, G.D. Westfall, C.K. Gelbke, L.H. Harwood, W.G. Lynch, D.K. Scott, H. Stöcker, M.B. Tsang and T.J.M. Symons, Phys. Rev Lett. 51 (1983) 1846.

[13] A. Breskin, R. Chechik and N. Zwang, Nucl. Instr. and Meth. 165 (1979) 125; IEEE Trans. Nucl. Sci. NS-27 (1980) 133.

[14] A. Breskin, Nucl. Instr. and Meth. 196 (1982) 11.

[15] J. van der Plicht and A. Gavron, Nucl. Instr. and Meth. 211 (1983) 403.

[16] C.R. Gruhn, M. Bimini, R. Legrain, R. Loveman, W. Pang, M. Roach, D.K. Scott, A. Shotter, T.J. Symons, J. Wouters, M. Zisman, R. de Vries, Y.C. Peng and W. Sondheim, Nucl. Instr. and Meth. 196 (1982) 33.

[17] Ch. Schiessl, W. Wagner, K. Hartel, P. Kienle, H.J. Korner, W. Mayer and K.E. Rehm, Nucl. Instr. and Meth. 192 (1982) 291.

[18] J.M. Asselineau, J. Duchon, M.L. Haridon, P. Mosrin, R. Regimbart and B. Tamain, Nucl. Instr. and Meth. 204 (1982) 109.

[19] R.J. McDonald, L.G. Sobotka, Z.Q. Yao, G.J. Wozniak and G. Guarino, Nucl. Instr. and Meth. 219 (1984) 508.

[20] A. Moroni, I. Iori, L.Z. Yu, G. Prete, G. Viesti, F. Gramegna and A. Danielli, Nucl. Instr. and Meth. 225 (1984) 57.

[21] L. Harwood, POISSON, private communication.

[22] D.H. Wilkinson, Rev. Sci. Instr. 23 (1952) 414.

[23] Harshaw, Inc., Solon, OH 44139, USA.

[24] Bicron, Inc., Newbury, OH 44065, USA.

[25] J.E. Yurkon et al., Conf. on Instrumentation for Heavy Ion Nuclear Research, Oak Ridge, TN (october 1984).

[26] C. Hurlbut, Bicron, Inc., private communication.